ACS OMEGA

Open Access



http://pubs.acs.org/journal/acsodf

Article

# *Trichoderma harzianum* Peptaibols Stimulate Plant Plasma Membrane $H^+$-ATPase Activity

Peter Klemmed Bjørk,* Nicolai Tidemand Johansen, Nanna Weise Havshøi, Silas Anselm Rasmussen, Johan Ørskov Ipsen, Thomas Isbrandt, Thomas Ostenfeld Larsen, and Anja Thoe Fuglsang*

Cite This: *ACS Omega* 2023, 8, 34928−34937

Read Online

ACCESS | Metrics & More | Article Recommendations | Supporting Information

**ABSTRACT:** Because of their ability to promote growth, act as biopesticides, and improve abiotic stress tolerance, *Trichoderma* spp. have been used for plant seed coating. However, the mechanism for the promotion of plant growth remains unknown. In this study, we investigate the effect of fungal extracts on the plant plasma membrane (PM) $H^+$-ATPase, which is essential for plant growth and often a target of plant-associated microbes. We show that *Trichoderma harzianum* extract increases $H^+$-ATPase activity, and by fractionation and high-resolution mass spectrometry (MS), we identify the activating components trichorzin PA (tPA) II and tPA VI that belong to the class of peptaibols. Peptaibols are nonribosomal peptides that can integrate into membranes and form indiscriminate ion channels, which causes pesticidal activity. To further investigate peptaibol-mediated $H^+$-ATPase activation, we compare the effect of tPA II and VI to that of the model peptaibol alamethicin (AlaM). We show that AlaM increases $H^+$-ATPase turnover rates in a concentration-dependent manner, with a peak in activity measured at 31.25 $\mu$M, above which activity decreases. Using fluorescent probes and light scattering, we find that the AlaM-mediated increase in activity is not correlated to increased membrane fluidity or vesicle integrity, whereas the activity decrease at high AlaM concentrations is likely due to PM overloading of AlaM pores. Overall, our results suggest that the symbiosis of fungi and plants, specifically related to peptaibols, is a concentration-dependent balance, where peptaibols do not act only as biocontrol agents but also as plant growth stimulants.

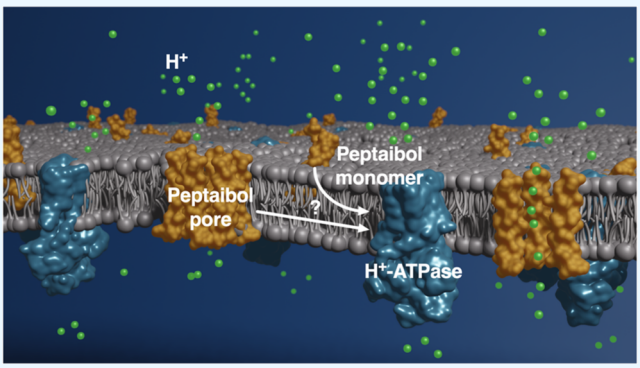


## INTRODUCTION

Crop yields are decimated by pathogens and pests[1] and crop loss is predicted to increase with changes in climate toward warmer and wetter conditions.[2] Fungi that stimulate plant growth or combat crop pathogens are potential biofertilizers and biopesticides, and a broad range of *Trichoderma* spp. have for decades been applied as seed coating.[3,4] They improve the fitness of germinating seeds and have been found to affect soil nutrient availability, plant immunity, and root architecture as well as to outcompete other microbes.[5] However, the finding that *Trichoderma* spp. can promote plant growth in optimal and sterile conditions suggests the existence of other plant-promoting effects.[6] *Trichoderma* spp.-induced plant growth can be triggered by fungal production of auxin species or fungal-induced *de novo* synthesis of auxin in plants.[6,7] However, not all *Trichoderma* spp. that produce auxin species promote plant growth and not all growth-promoting *Trichoderma* spp. produce auxin.[8] This points toward another and more complex explanation for the plant growth promotion observed after *Trichoderma* spp. treatment.

*Trichoderma* spp. produce a range of peptaibols, which are linear peptides, approximately 5−21 amino acids in length.[9,10] More than 300 different peptaibols have been reported (http://peptaibol.cryst.bbk.ac.uk/home.shtml), and, in general, they form $\alpha$-helices that span the membrane and congregate into a barrel-stave pore structure with polar regions orientated toward the pore interior, creating an indiscriminate ion channel.[9−12] Besides the antibiotic activity, peptaibols have been demonstrated to be a signal molecule for fungus-growing ants to weed out pieces of their fungal garden compromised by *Trichoderma* spp.[13] The peptaibol alamethicin (AlaM) is commonly used to study pore formation in membranes and serves as a molecule of choice for several biophysical studies on peptide integration into membrane systems.[12,14] Most studies employ artificial membranes, but several biological membranes are also affected by AlaM treatment.[15] Emerging evidence suggests that plant plasma membrane (PM) heterogeneity has

Received: June 16, 2023
Accepted: August 16, 2023
Published: September 14, 2023

a pronounced effect on how peptaibols integrate into the membrane, and insight gained on model membranes does not necessarily apply to natural membranes.[16]

Although several modes of action have been hypothesized, the effect of peptaibols in plants remains elusive. *Trichoderma asperellum* has been shown to induce growth in maize seedlings, and it was suggested that activation of the PM $H^+$-ATPase was the cause.[17] There, *T. asperellum* extracellular extract was shown to differentially activate the PM $H^+$-ATPase compared to the auxin species indole-acetic acid (IAA). This result is in line with the finding that not all auxin-producing *Trichoderma* spp. promote plant growth and vice versa,[8] and it suggests that unknown specialized *Trichoderma* metabolites promote plant growth through stimulation of the plant PM $H^+$-ATPase.

In this study, we used a bioassay-guided approach to identify secreted fungal metabolites with the potential to modulate plant PM $H^+$-ATPase activity. By analyzing the effect of the total secreted metabolites on PM ATP hydrolysis, we identified active metabolites from *Trichoderma harzianum*. Extracts that gave rise to changes in ATP hydrolysis were further fractionated and assayed for their effect on ATP hydrolysis. By this approach, we were able to identify a range of peptabols from *T. harzianum* that were potent activators of $H^+$-ATPase activity. Among the compounds, we identified two major groups of peptaibols with structural similarity to the well-studied model peptaibol AlaM. AlaM was found to have a similar effect on $H^+$-ATPase activity, and we further studied the effect of AlaM on tight plant PM vesicles. By a combination of biophysical and biochemical experiments, we found that the increased ATPase activity was correlated to AlaM insertion in the PM. These observations suggest that *Trichoderma* targets the PM $H^+$-ATPase via peptaibols. Future studies on the integration of AlaM and other peptaibols into natural membranes must therefore consider how the interplay between membrane proteins, their lipid environment, and peptaibols affects the membrane.

## MATERIALS AND METHODS

**Chemical Materials.** Alamethicin (AlaM) (catalog no. 27061-78-5) was purchased from both Santa Cruz Biotechnology (Dallas, Texas) and Sigma-Aldrich (St. Louis, Missouri). No differences were detected in the biological assays.

**Purification of Spinach Plasma Membranes.** Plasma membrane (PM) vesicles from *Spinicia oleracea* were isolated using two-phase partitioning as described by Lund and Fuglsang.[18] Briefly, 30−75 g of fresh *S. oleracea* (baby spinach) leaves were homogenized in buffer (50 mM MOPS, 5 mM EDTA, 50 mM $Na_4P_2O_7$, 0.33 M sucrose, 1 mM $Na_2MoO_4$, pH 7.5) and centrifuged at 10 000*g* for 15 min. The supernatant was collected and centrifuged at 50 000*g* for 30 min, and the pellet was resuspended in 330/5 buffer (0.33 M sucrose, 5 mM $K_2HPO_4$ pH 7.8). The resuspended pellet was added on top of a two-phase partitioning buffer (6.2% Dextran T500 solution, 6.2% PEG4000, 0.33 M sucrose, 5 mM $K_2HPO_4$ pH 7.8, 3 mM KCl) and centrifuged at 1000*g* for 5 min. The plasma membrane phase was collected and centrifuged at 100 000*g* for 1 h. The pellet was collected and resuspended in a 330/5 buffer. The protein concentration was determined using a Bradford colorimetric assay,[19] and the PM fractions were frozen in liquid $N_2$ and stored at −80 °C until use.

**Fungal Cultivation and Fractionation.** Species *Alternaria gaisen* (IBT BA 938), *Alternaria turkisafria* (IBT BA 927), *Fusarium aveneaceum* (IBT 41708), *Fusarium oxysporum* (IBT 40467), *Fusarium poae* (IBT 40485), and *T. harzianum* (IBT 41414) were grown on potato dextrose agar (PDA), malt extract agar (MEA), and yeast extract with supplement (YES) plates for 10−14 days at 25 °C in the dark. Fungal material was then harvested and extracted with ethyl acetate containing 0.5% (v/v) formic acid. The extracts were concentrated in vacuo. *T. harzianum* gave rise to the highest activation in the ATPase assay and was selected for further examination. Large-scale *T. harzianum* extract was initially fractionated on diol-functionalized silica (Biotage, Uppsala, Sweden) by using an Isolera autoflasher (Biotage, Uppsala, Sweden). The column was eluted stepwise using heptane, dichloromethane, ethyl acetate, and methanol in 50% increments. The active fractions were pooled and taken through another round of fractionation using a C18-packed column. Fractions were eluted using a stepwise gradient of A (50 ppm trifluoroacetic acid), and B (methanol, 50 ppm trifluoroacetic acid), from 10% methanol to 100% methanol in increments of 10% methanol, using an Isolera autoflasher (Biotage, Uppsala, Sweden), with each fraction being three column volumes (45 mL).

**UHPLC−DAD−HRMS.** Extracts and fractions were analyzed by ultrahigh-performance liquid chromatography−diode array detection−high-resolution mass spectrometry (UHPL−DAD−HRMS) using a 1290 Infinity UHPLC machine (Agilent, Santa Clara, California). Separation was achieved on a 2.0 ′ 150 mm Poroshell phenyl-hexyl column (2.7 Å; Agilent Technologies, Santa Clara, California). The column was eluted with a linear gradient consisting of A (20 mM formic acid) and B (acetonitrile, 20 mM formic acid) starting at 10% B and increasing to 100% B over 15 min and held at this composition for 2 min before returning to initial conditions. MS detection was performed by a 6540 series quadropole time-of-flight (QTOF) mass spectrometer equipped with a dual jet stream electrospray ionization (ESI) source operating in positive mode. Data-dependent auto MS/MS acquisition was performed using fixed collision-induced dissociation (CID) collision energies of 10, 20, and 40 eV. The data generated were dereplicated employing an in-house MS/HRMS natural product database.[20]

**ATPase Assay.** $H^+$-ATPase activity was assayed according to a modified protocol of the Baginski assay,[21] as described by Wielandt et al.[22] In a 96-well plate, 1−3 $\mu$g of protein was added in 60 $\mu$L volumes per well. The assay was performed at 30 °C for 30 min, with 2.5 mM ATP, pH 7 in ATPase buffer (20 mM MOPS pH 7, 8 mM $MgSO_4$, 50 mM $KNO_3$, 5 mM $NaN_3$, 0.25 mM $Na_2MoO_4$), and stopped by addition of ice-cold stop solution (100 mM ascorbic acid, 0.3 M HCl, 0.05% sodium dodecyl sulfate (SDS), 5 mM $(NH_4)_6Mo_7O_{24}$). Samples were incubated for 15 min on ice before addition of 75 $\mu$L $NaAsO_2$. Absorbance was measured at 860 nm using a SpectraMax M5 microplate reader (Molecular Devices, San Jose, California) to quantify the amount of phosphomolybdate generated from hydrolyzed ATP. For kinetics studies, the concentration of ATP was varied as described in the text with an ATP-regenerating system (5 mM phosphoenolpyruvate, 0.05 $\mu$g/$\mu$L pyruvate kinase). Fungal extracts, isolated peptaibols, AlaM, fluorescent probes DPH, and TMA-DPH were added to wells prior to PM addition and assay start unless otherwise stated in the text.


https://doi.org/10.1021/acsomega.3c04299
ACS Omega 2023, 8, 34928−34937

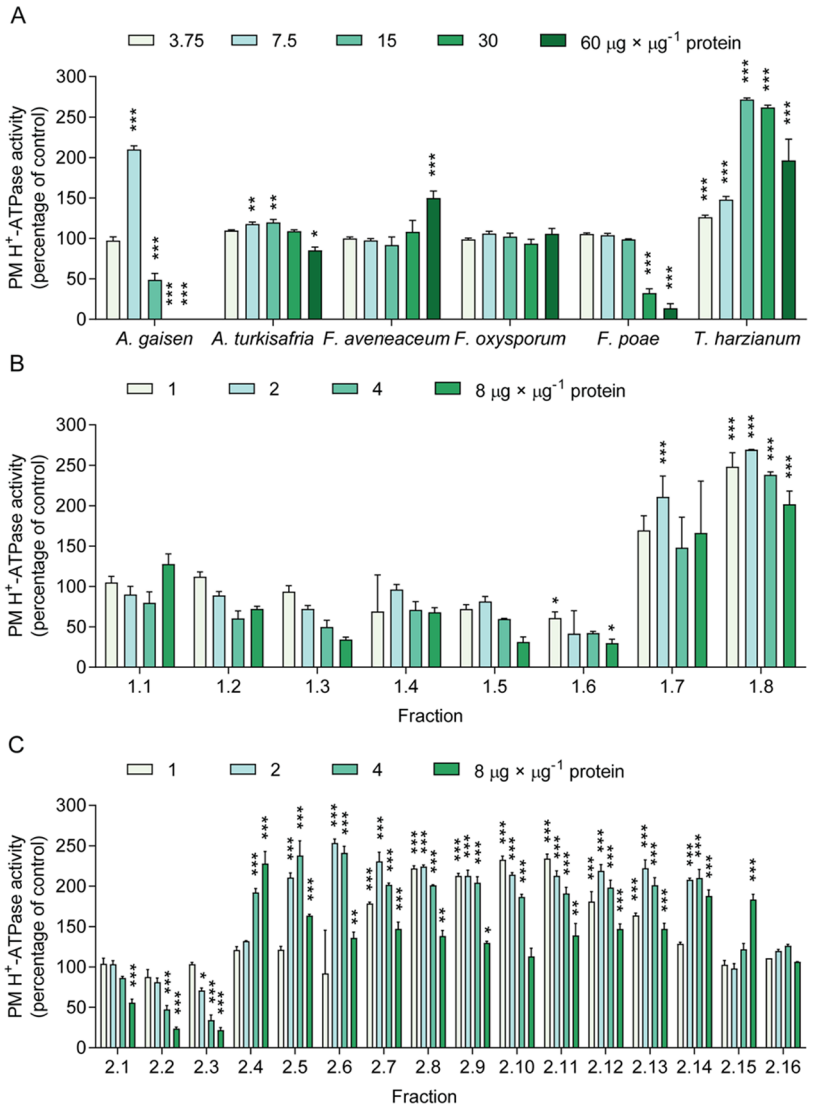


**Figure 1.** Effect of fungal extracts on ATP hydrolysis of the plant plasma membrane $H^+$-ATPase. (A) ATP hydrolysis of the *S. oleracea* plasma membrane (PM) $H^+$-ATPase was assayed in response to an increasing concentration of extract from six plant-associated fungi. (B) Metabolites extracted from *T. harzianum* (from panel (A)) were further separated into eight new fractions (1.1−1.8), and the effect on ATP hydrolysis was assayed again. (C) Fraction 1.8 (from panel (B)) was further fractionated into 16 fractions (2.1−2.16), and the effect on ATP hydrolysis was assayed in response to increasing concentrations. Data are shown as mean ± SEM ($n$ = 3) and are representative of metabolites from fungi from two independent growth and fractionation events. Data were analyzed by two-way analysis of variance (ANOVA) and ATP hydrolysis was compared to ATP hydrolysis of the control (DMSO treated, not shown) with a Bonferroni post-test: * = $P < 0.05$; ** = $P < 0.01$; *** = $P < 0.001$.

**$H^{\pm}$ Pumping Assay.** *S. oleracea* plasma membrane vesicles were turned inside out using the detergent Brij 58.[23] $H^+$ transport across the membrane was assayed by a modified version of the method described by Lund and Fuglsang.[18] Quenching of the fluorescent probe, 9-amino-6-chloro-2-methoxyacridine (ACMA) was assayed by excitation at 412 nm, and emission was measured at 480 nm. The assay was performed using 2.5 $\mu$g protein per well in 96-well plates or 16.7 $\mu$g protein in 1 mL cuvettes, depending on equipment availability, in reaction buffer (11.4 mM MOPS, 56.8 mM $K_2SO_4$, 22.7 mM glycerol, 2.3 mM ATP, 1 $\mu$M ACMA, 0.05% Brij 58, 60 nM valinomycin, pH 7.0) and started by addition of $MgSO_4$ to a final concentration of 3 mM. The assay was stopped by addition of 10 $\mu$M of the $H^+$ ionophore, nigericin. Fungal extracts, isolated peptaibols, AlaM, and fluorescent probes, DPH and TMA-DPH, were added to wells prior to PM addition and assay start unless otherwise stated in the text.

**Fluorescence Polarization.** Fluorescent probes 1,6-diphenyl-1,3,5-hexatriene (DPH, Sigma-Aldrich) and *N,N,N*-trimethyl-4-(6-phenyl-1,3,5-hexatrien-1-yl)phenylammonium (TMA-DPH, Sigma-Aldrich) were dissolved in dimethyl sulfoxide (DMSO) to a concentration of 10 mM. Stocks of 0.1 mM were prepared by dilution in DMSO. Samples were essentially set up as for ATPase assays, but with the exception that the fluorescent probes were added to a final concentration of 0.1 $\mu$M followed by 30 min incubation at 30 °C to ensure incorporation of the probes. Fluorescence was measured on 100 $\mu$L samples in a black quartz cuvette (Hellma, Müllheim, Germany) with a 90° window using a Horiba FluoMax-4 spectrofluorometer (Horiba, Kyoto, Japan) equipped with a temperature control unit set to 30 °C. For both probes, the excitation wavelength was 350 nm, the emission wavelength was 428 nm, and the integration time was 1 s. For DPH, the


https://doi.org/10.1021/acsomega.3c04299
ACS Omega 2023, 8, 34928−34937

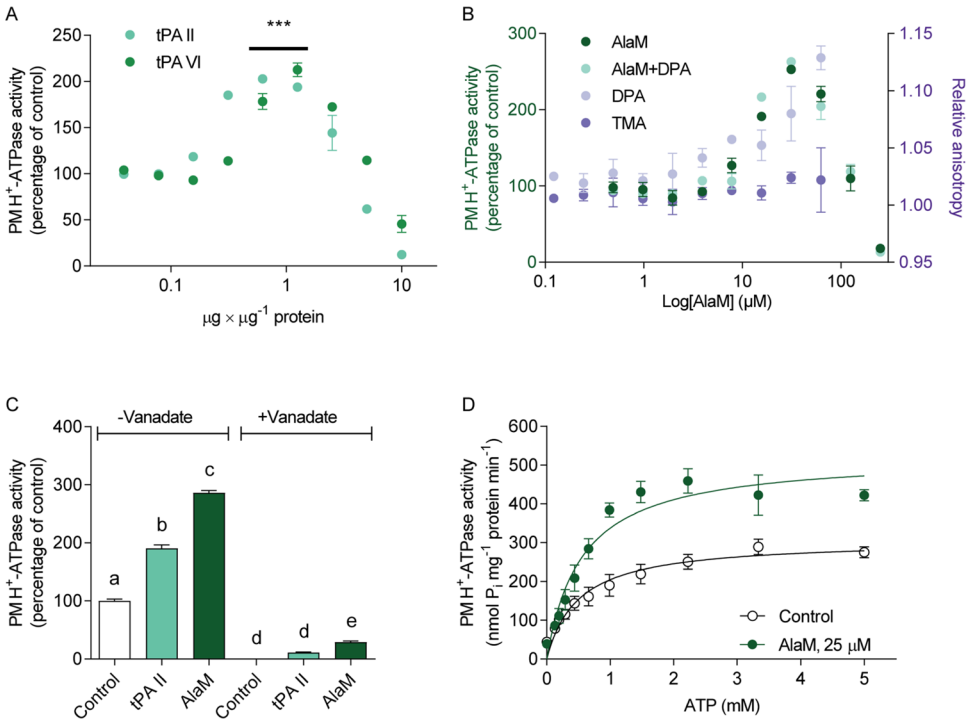


**Figure 2.** ATP hydrolysis of the *S. oleracea* plasma membrane $H^+$-ATPase in response to tPA II, tPA VI, AlaM. (A) Effect of *T. harzianum*-derived peptaibols, tPA II and tPA VI, and (B), commercial alamethicin on plant plasma membrane (PM) $H^+$-ATPase activity were tested at increasing concentrations and compared to a control treated with DMSO. Values are mean ± SEM ($n$ = 3) and are representative of two independent experiments. Activity was analyzed by one-way analysis of variance and compared to ATP hydrolysis of the control by a Dunnett's multiple comparisons test; *** = $P < 0.001$. (C) ATP hydrolysis of plant PM $H^+$-ATPases treated with tPA II (0.05 $\mu$g/$\mu$L) or AlaM (0.05 $\mu$g/$\mu$L) and vanadate, a PM $H^+$-ATPase inhibitor. Values are mean ± SEM ($n$ = 3) and are representative of two independent experiments. ATP hydrolysis with and without vanadate was analyzed using one-way ANOVA and compared to ATP hydrolysis of the control by a Bonferroni post-test. Different letters are used to indicate means that differ significantly ($P < 0.05$). (D) Kinetic analysis was performed by plotting specific activity as a function of ATP concentration (mM) in response to treatment with 25 $\mu$M AlaM. Values are mean ± SEM of four technical replicates of two independent PM fractionations ($n$ = 8).

excitation and emission slit widths were 5 nm, whereas for TMA-DPH, they were 7.5 nm.

**Dynamic and Static Light Scattering.** Samples were prepared under conditions identical to those of the ATPase assay but in a volume of 900 $\mu$L per sample. Each sample was transferred to a quartz cuvette (Hellma, Müllheim, Germany) and centrifuged at 4000*g* for 5 min to remove eventual traces of dust or very large aggregates. Light scattering was measured on a BI-200SM instrument (Brookhaven Instruments, Holtsville, New York) equipped with a diode laser emitting light with a wavelength of 637 nm. The detector was placed at 90° to the incoming light, and the temperature inside the VAT was kept at 30 ± 0.1 °C by an external water bath. Data frames of 30 s were collected continuously over the course of 20 min. The static signal is proportional to the weight-average molecular weight of the measured species as described elsewhere.[24] *Z*-average hydrodynamic diameters were calculated from the dynamic light scattering signal by using the quadratic cumulant fit in the instrument software. The reported standard deviations were calculated from the diameters.

**Statistics.** All biochemical experiments were performed at least in triplicate and repeated three times unless fungal extract availability prohibited so. Values are presented as mean ± standard error of the mean (SEM), *P*-values were calculated by one- or two-way analysis of variance (ANOVA) followed by Dunnett's post-test analysis or Bonferroni post-test using GraphPad Prism 9.3. $P < 0.05$ was considered statistically significant. *, $P < 0.05$; **, $P < 0.01$; ***, $P < 0.001$. The kinetic parameters, $V_{max}$, $K_m$, were estimated by nonlinear regression using GraphPad Prism 5.0a.

## RESULTS

***T. harzianum* Extract Stimulates Plant PM $H^+$-ATPase ATP Hydrolysis.** Using an ATP hydrolysis assay, we screened six plant-associated fungi for their effect on the plant PM $H^+$-ATPase activity. This group of fungi contained five pathogens: *A. gaisen*, *A. turkisafria*, *Fusarium avenaceum*, *F. oxysporum*, *F. poae*, and one beneficial fungus, *T. harzianum*. The effect of the fungal extract on $H^+$-ATPase activity was tested at ratios of 3.75−60 $\mu$g of extract per $\mu$g of protein, at a final protein concentration of 1/60 $\mu$g/$\mu$L. Figure 1A shows the measured ATPase activity normalized to control treatment with DMSO. The extracts are from *A. gaisen*, *A. turkisafrie*, *F. avenaceum*, *F. oxysporum*, and *F. poae* had little or inconsistent effects on ATP hydrolysis, whereas metabolites extracted from *T. harzianum* significantly increased ATP hydrolysis of the $H^+$-ATPase for all but the highest ratio tested (60 $\mu$g of extract per $\mu$g protein). As such, several of the tested fungi had an effect on the ATPase activity, but only *T. harzianum* was identified as a consistent modulator of the plant $H^+$-ATPase. To identify the metabolite(s) responsible for increased ATP hydrolysis, extracts from *T. harzianum* was selected for further


https://doi.org/10.1021/acsomega.3c04299
ACS Omega 2023, 8, 34928−34937

fractionation by liquid flash chromatography and reversed-phase high-performance liquid chromatography (RP-HPLC).

***T. harzianum* Modulates H$^+$-ATPase Activity through Production of Peptaibols.** The extracted metabolites from *T. harzianum* were separated into eight fractions, here named 1.1−1.8 (Figure 1B). Fractions 1.1−1.8 were screened for their effect on ATP hydrolysis at ratios of 1, 2, 4, and 8 $\mu$g of extract per $\mu$g protein. No changes in activity were observed for fractions 1.1−1.6, but fraction 1.7, at 2 $\mu$g per $\mu$g protein, and fraction 1.8 significantly increased ATP hydrolysis. Fraction 1.8 increased H$^+$-ATPase activity at a lower ratio than observed in the initial screening, suggesting a high specific modulatory activity. ATP hydrolysis peaked at approximately 270% of control when PM fractions were treated with 2 $\mu$g of extract per $\mu$g of protein of fraction 1.8, while 8 $\mu$g of extract per $\mu$g of protein resulted in an ATPase activity of 200% of control (Figure 1B). To further pinpoint the activating metabolite(s), fraction 1.8 was separated by RP-HPLC, resulting in 16 fractions (2.1−2.16) (Figure 1C). This time, the ATPase activating effect was scattered over 11 different fractions, suggesting that active metabolite(s) could not be effectively separated by the employed method (Figure 1C). UHPLC−DAD−HRMS analysis of the 11 fractions revealed that all fractions contained a mix of peptaibols.

**Peptaibols Stimulate ATP Hydrolysis of the Plant PM H$^+$-ATPase.** It was possible to separate the peptaibols into two fractions: a homogeneous sample of the peptaibol, trichorzin PA VI (tPA VI), and a rather heterogeneous sample dominated by the peptaibol, trichorzin PA II (tPA II) (Duval et al., 1997).[25] Henceforth, these fractions are referred to as tPA VI and tPA II. Both tPA VI and tPA II were found to increase ATP hydrolysis to >200% of control at a ratio of 1.25 $\mu$g trichorzin per $\mu$g protein, corresponding to a concentration of ∼10 $\mu$M trichorzin (Figure 2A). Increasing the trichorzin concentration above this point resulted in an inhibitory effect, where the ATP hydrolysis declined to 10−30% of the control at 10 $\mu$g of trichorzin per $\mu$g protein.

To evaluate if this observed effect on the PM H$^+$-ATPase was common for peptaibols or limited to trichorzins, we included the well-studied model peptaibol AlaM, which was obtained commercially. AlaM was found to stimulate ATP hydrolysis of PM H$^+$-ATPase in the same pattern as observed for tPA VI and tPA II, and the maximum activation was observed at 25 $\mu$M AlaM (Figure 2B). Higher concentrations of AlaM resulted in PM H$^+$-ATPase inhibition, consistent with the effects observed for tPA II and tPA VI (Figure 2A). AlaM concentrations above 9.5 $\mu$M per $\mu$g of protein significantly increased H$^+$-ATPase activity compared to the control (Figure 2B).

To confirm that the observed ATP hydrolysis was caused by trichorzin- or AlaM-induced activation of the PM H$^+$-ATPase, protein samples were treated with the PM H$^+$-ATPase inhibitor, vanadate. To induce H$^+$-ATPase activation, vesicles prepared from plant PM were treated with 0.05 $\mu$g/$\mu$L of tPA II or AlaM, corresponding to 24.8 and 25.5 $\mu$M, respectively (Figure 2C). Peptaibol treatment alone increased H$^+$-ATPase activity 2−3-fold compared to the control for tPA II and AlaM, respectively, while 5 mM vanadate treatment abolished the ATP hydrolysis (Figure 2C). These results confirm that both tPA II purified from *T. harzianum*, and commercial AlaM activate ATP hydrolysis of the PM H$^+$-ATPase and show that peptaibol activation of the H$^+$-ATPase is sensitive to vanadate treatment.

To further characterize the mechanism behind peptaibol-mediated H$^+$-ATPase activation, we assayed the effect of increasing the ATP concentration while keeping the AlaM concentration constant (Figure 2D). $K_m$ for the AlaM treated samples was 0.55 mM ATP, which was the same as for the control sample that had a $K_m$ of 0.50 mM ATP. The maximum velocities, $V_{max}$, were determined to be 525 and 307 nmol $P_i$ × mg protein$^{-1}$ × min$^{-1}$ for the PM fractions treated with AlaM and control, respectively (Table 1). Kinetic values and their corresponding standard errors are summarized in Table 1. These results indicate that AlaM has no effect on the substrate affinity of the PM H$^+$-ATPase, but it increases the turnover rate.

**Table 1. Effect of Alamethicin on $K_m$ and $V_{max}$ of the Plant Plasma Membrane H$^+$-ATPase**

| | $K_m$ (mM ATP) | $V_{max}$ (nmol $P_i$/mg/min) |
|---|---|---|
| control | 0.50 ± 0.09 (SE) | 306.8 ± 16.4 (SE) |
| AlaM, 25 $\mu$M | 0.55 ± 0.09 (SE) | 524.6 ± 26.7 (SE) |

ATP hydrolysis of *S. oleracea* plasma membrane (PM) fractions were measured at increasing ATP concentration in response to in vitro treatment with alamethicin (AlaM) and *T. harzianum* extract. The enzyme kinetic parameters, $K_m$ and $V_{max}$, were determined from nonlinear regression of the Michealis−Menten equation and are shown with standard errors (SE). Values are determined based on four technical replicates of two independent PM fractions ($n$ = 8).

**AlaM-Mediated PM H$^+$-ATPase Activation Is Not due to Increased Membrane Fluidity.** Modulation of ATPase turnover rates has previously been linked to changes in membrane fluidity.[26,27] To evaluate membrane fluidity in PM vesicles, we measured the fluorescence anisotropy of two fluorescent probes, DPH and TMA-DPH. DPH integrates into the hydrophobic interior of a lipid bilayer, while TMA-DPH integrates more toward the polar headgroup region of a lipid bilayer. DPH and TMA-DPH did not affect ATP hydrolysis (Figure S1A) or H$^+$ pumping of the PM H$^+$-ATPase (Figure S1B,C,D) in concentrations up to 10 times higher than used for fluorescence anisotropy (0.1 $\mu$M). Figure 2B shows the measured anisotropy as a function of the AlaM concentration relative to a control sample without AlaM added. A small but steady increase in DPH anisotropy could be detected at AlaM concentrations above ∼10 $\mu$M, coinciding with the onset of increased ATPase activity, whereas the relative anisotropy of TMA-DPH was virtually unaffected by the addition of AlaM (Figure 2B). However, at 62.5 $\mu$M AlaM, the trend of increased DPH anisotropy was uncoupled from that of the ATPase activity profile (Figure 2B). These results suggest that AlaM, above a given concentration threshold, reduces membrane fluidity in the central part of the bilayer of PM vesicles while the headgroup region of the membrane is unaffected. In turn, this indicates that AlaM inserts into the membrane, as expected.

**AlaM Pores in the PM Results in Collapse of the Membrane Potential.** To confirm that the observed increase in ATP hydrolysis was due to PM H$^+$-ATPase activation, the rate of H$^+$ pumping was measured using the fluorescent probe 9-amino-6-chloro-2-methoxyacridine (ACMA). The H$^+$ pumping rate was quantified by measuring fluorescence quenching for inside-out vesicles treated with concentration ratios ranging from 0.5 to 15 $\mu$M AlaM per $\mu$g of protein (Figure 3A,B). The


https://doi.org/10.1021/acsomega.3c04299
ACS Omega 2023, 8, 34928−34937

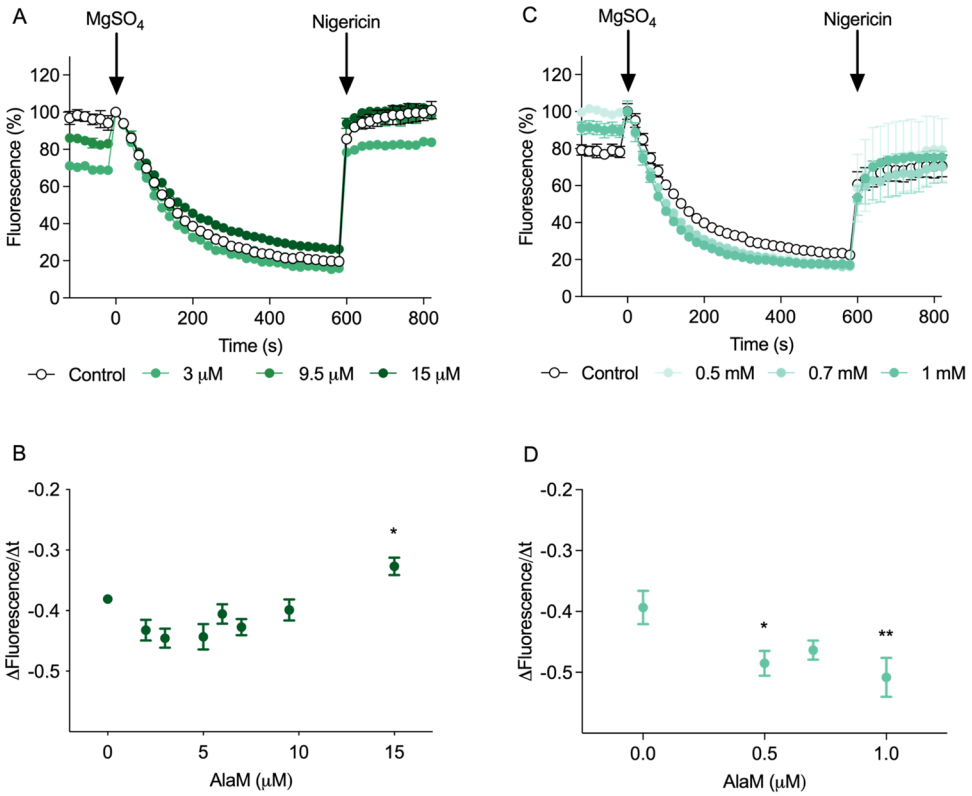


**Figure 3.** Alamethicin effect on the $H^+$ pumping of plasma membrane vesicles. Accumulation of $H^+$ in inside-out plasma membrane (PM) vesicles treated with (A) 2−15 $\mu$M and (C) 0.5−1.0 $\mu$M AlaM was quantified using the fluorescent probe ACMA. The assay is activated by addition of $MgSO_4$ and stopped by addition of the $H^+$ ionophore, nigericin. (B, D) Fluorescence quenching from $t$ = 0 to $t$ = 120 (initial rate) was analyzed using linear regression, and the slopes were plotted as a function of AlaM concentration. Values are mean ± SEM ($n$ = 3) and are representative of two independent experiments. Data were analyzed using one-way analysis of variance (ANOVA), and Dunnet's multiple comparisons test was used to calculate the difference in slopes compared to the control: * = $P$ < 0.05; ** = $P$ < 0.01.

initial pumping rates (from $t$ = 0 s to $t$ = 120 s) were extracted by linear fits and compared between samples. At 15 $\mu$M AlaM, the $H^+$ pumping rate was significantly reduced (Figure 3B), but rates 0 < 5 $\mu$M AlaM indicated that $H^+$ pumping could be increased at lower concentrations. $H^+$ pumping was therefore investigated at lower concentrations (Figure 3C), and we found that rates were significantly increased for plant PM vesicles treated with 0.5 or 1.0 $\mu$M AlaM (Figure 3D). This observation corresponds to previous results, which showed that AlaM initially increased $H^+$-ATPase activity before inhibiting activity (Figure 2B). However, the threshold concentrations for activation and inhibition were different for the ATPase activity assay and $H^+$ pumping assay. This effect can be explained by the formation of AlaM pores in the PM vesicles already below 15 $\mu$M. AlaM pores are reported to function as ion channels. When either protons or potassium ions are allowed through the pore, the membrane potential will be reduced or even collapsed. Thereby, the $H^+$ pumping assay that requires tight vesicles is not viable under this condition. This is in contrast to the ATPase assay that does not require a tight vesicle. Alternatively, at high AlaM concentrations, the AlaM/lipid ratio in the membrane might be so high that the PM $H^+$-ATPase gets devoid of native lipid contacts or AlaM directly affects the protein and thereby the ATPase activity as well. Finally, the abolished $H^+$ pumping could be caused by vesicle breakage due to the high AlaM concentrations. However, the latter does not seem to be the case as analysis of the PM vesicles by dynamic light scattering (DLS) and static light scattering (SLS) showed that the average diameters and count rates were rather stable up to 62.5 $\mu$M AlaM (Figure S2). This suggests that vesicles remain intact in the region of $H^+$-ATPase activation, 10−62.5 $\mu$M (Figure 2B). At AlaM concentrations > 62.5 $\mu$M, the DLS-derived diameters start increasing, suggesting a change to vesicle integrity. Following this observation, we explain the steady decrease in membrane fluidity and the decreasing $H^+$-ATPase activity at very high AlaM concentrations (Figure 2B) to overloading of AlaM pores and potentially the disruption or collapse of PM vesicles.

## DISCUSSION AND CONCLUSIONS

Peptaibols are the predominant specialized metabolites produced by many distinct types of *Trichoderma* spp., including *T. harzianum*.[28−30] The fungicidal and antiviral effects of peptaibols have been described extensively, and *Trichoderma* spp. have been applied as commercial biocontrol agents, primarily based on these effects.[28,31] However, *T. harzianum* has also been shown to stimulate plant growth and many different growth-activating mechanisms have been proposed, including activation of the plant PM $H^+$-ATPase.[17] In this study, we identified peptaibol trichorzins PA II and VI as the main PM $H^+$-ATPase activating component of *T. harzianum* extract, which agrees with the results reported by Lopez-Coria et al.[17] We compared the $H^+$-ATPase stimulating effect of peptaibols isolated from *T. harzianum* with AlaM and found a similar response. These observations lead us to hypothesize that peptaibols act not simply as biocontrol agents


https://doi.org/10.1021/acsomega.3c04299
ACS Omega 2023, 8, 34928−34937

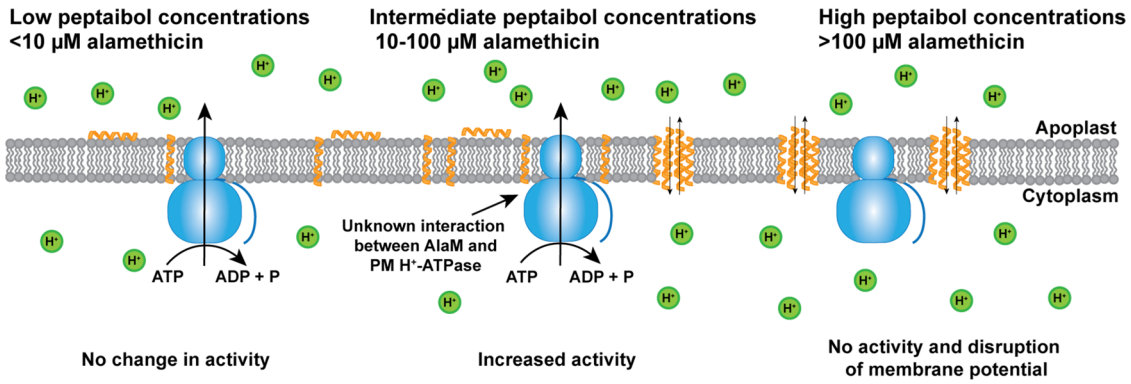


**Figure 4.** Model of peptaibol insertion into plant plasma membrane vesicles. Peptaibol molecules in concentrations of <5 $\mu$M interact with the membrane but show little to no effect on plasma membrane (PM) $H^+$-ATPase activity and membrane stability. Peptaibol molecules in concentrations of 5−30 $\mu$M integrate into the PM and activate the PM $H^+$-ATPase directly or indirectly through an unknown mechanism. Peptaibol molecules in concentrations > 30 $\mu$M integrate into the PM and create indiscriminative ion channels, leading to disruption of the membrane.

but also as a plant growth stimulant, further expanding the interaction between plants and *Trichoderma* spp.

$H^+$ pumping proved to be more ambiguous in response to AlaM. The literature provides numerous examples of peptaibol integration into artificial membranes and aggregation of peptaibol to create pores. Many of these examples have been thoroughly reviewed.[9,15,32,33] It was therefore anticipated that peptaibols would render the PM vesicles permeable to $H^+$, collapsing the membrane potential, and any measured $H^+$ pumping in the ACMA assay would be masked by a simultaneous leakage from peptaibol pores. In agreement with this prediction, initial experiments showed that peptaibols inhibited $H^+$ pumping ∼ 15 $\mu$M (Figure 3A,B). However, decreasing the peptaibol concentration suggested that a small dosage of AlaM increased the rate of $H^+$ pumping in the ACMA assay (Figure 3C,D). We observed a significant increase in $H^+$ pumping in response to 0.5 and 1.0 $\mu$M AlaM, while 15 $\mu$M AlaM significantly decreased the level of $H^+$ pumping. The increase in $H^+$-ATPase-mediated $H^+$ pumping after treatment with AlaM was not comparable to the increase observed in ATP hydrolysis experiments (Figure 2B). This can be explained by a model in which AlaM-induced $H^+$ influx is rapidly surpassed by $H^+$ leaking out as the AlaM concentration is increased. An assay that measures ATP hydrolysis is unaffected by this because pores in an otherwise intact membrane are not expected to affect ATP hydrolysis. Increasing this concentration leads to peptaibol aggregation and pore formation. The increase in $H^+$ pumping is therefore detectable only under these assay conditions when peptaibols are added in concentrations ranging from 0 to 1 $\mu$M (Figure 3C,D).

*Trichoderma* spp. have shown antimicrobial activity and are widely considered to be beneficial fungi in plant growth. However, the mechanisms leading to growth promotion are poorly understood.[34−36] Many *Trichoderma* spp. produce auxin-like compounds, but this alone cannot explain plant growth promotion.[8] The antimicrobial activity of *Trichoderma* spp. is explained by production of a range of antimicrobial compounds, and especially the pore-forming peptaibols.[8,34] Peptaibols seem to be both stimulating and detrimental to plant growth,[37] and the question remains: how do plants tolerate peptaibols in natural conditions? The integration of peptaibols into membranes with a heterogeneous lipid composition remains to be thoroughly described, and evidence has emerged, demonstrating that peptaibols are not inserted and aggregated into pores equally in all lipid environments.[16,38,39] It was demonstrated that the peptaibol concentration needed for pore formation in plant PMs increases upon exposure of the plants to cellulases. Exposure to minute concentrations of *T. viride* cellulases renders plant PM more tolerant to AlaM-induced permeability by redistribution of lipids in the membrane.[16,38,40] However, we cannot know whether this increased tolerance is caused by AlaM not being inserted into the membrane or if AlaM is inserted without forming pores. Dotson et al. found that cellulase-induced lipid distribution in the plant PM inhibited formation of AlaM pores, suggesting that AlaM pores are not formed equally well in all lipid environments. From the available data, it cannot be distinguished whether AlaM is inserted into the cellulase-treated PM and not forming pores or if AlaM is not inserted into the PM before the concentration reaches a certain threshold.[41] Bertelsen et al. showed that AlaM integrates differently in different lipid environments,[39] supporting the finding that changes to the PM composition can lead to AlaM tolerance. Analysis of the membrane composition showed that tolerant cells had membranes enriched in phosphatidylethanolamine and phosphatidylglycerol, while phosphatidylserine and phosphatidylinositol were decreased compared to the control.[38] $H^+$-ATPase activity is affected by lipid composition,[42] and it is not fully understood how lipid redistribution in response to cellulases changes $H^+$-ATPase activity *in planta*. Further studies are needed to investigate the mechanism of peptaibol pore formation in membranes that resemble the plant PM.

We found that ATP hydrolysis peaked in response to a concentration of 1.25 $\mu$g (ca. 25 $\mu$M) per $\mu$g of protein for the *T. harzianum*-derived peptaibols, tPA II and tPA VI, and the well-studied peptaibol, AlaM. This concentration corresponds well to the concentrations used in other studies of peptaibol effect in plants.[16,37,38] However, to describe the effect of peptaibols more accurately *in planta*, their concentration in the root zone must be established.

The present study provides evidence that peptaibols increase $H^+$-ATPase activity, and this may be involved in *Trichoderma* spp. promoted plant growth. Based on available literature and present data, we propose that peptaibols integrate stably into plant PM and activate the plant PM $H^+$-ATPase (Figure 4). The ability of peptaibols to aggregate into pores has been


https://doi.org/10.1021/acsomega.3c04299
ACS Omega 2023, 8, 34928−34937

shown to be highly susceptible to peptaibol concentration and lipid composition, and we did not find that peptaibols affected overall vesicle integrity until added in concentrations higher than 62.5 $\mu$M (Figure S2). The peptaibol AlaM decreased the membrane fluidity, as measured by DPH anisotropy, above a given concentration threshold, which coincided with the onset of ATPase activation above the basic level. While other ATPases have been described to be activated by increased membrane fluidity,[43] we find that changes in membrane fluidity are not the main driver of PM $H^+$-ATPase activation by AlaM. The effect on plant roots in soil is therefore dependent on the concentration of peptaibols and changes in the lipid composition of the PM of live root cells. Both questions need further research before it can be evaluated whether peptaibols are growth inhibitors or promoters under natural conditions.

## ■ ASSOCIATED CONTENT

### Supporting Information

The Supporting Information is available free of charge at https://pubs.acs.org/doi/10.1021/acsomega.3c04299.

Control experiments showing that DPH have no effect on ATPase and $H^+$ pumping, and effect of AlaM on vesicle size and integrity (PDF)

## ■ AUTHOR INFORMATION


### Corresponding Authors

**Peter Klemmed Bjørk** − *Department of Plant and Environmental Sciences, Faculty of Science, University of Copenhagen, 1871 Frederiksberg, Denmark;* orcid.org/0000-0002-5641-7791; Email: pkbj@plen.ku.dk

**Anja Thoe Fuglsang** − *Department of Plant and Environmental Sciences, Faculty of Science, University of Copenhagen, 1871 Frederiksberg, Denmark;* orcid.org/0000-0003-1153-8394; Email: atf@plen.ku.dk

### Authors

**Nicolai Tidemand Johansen** − *Department of Plant and Environmental Sciences, Faculty of Science, University of Copenhagen, 1871 Frederiksberg, Denmark;* orcid.org/0000-0002-8596-548X

**Nanna Weise Havshøi** − *Department of Plant and Environmental Sciences, Faculty of Science, University of Copenhagen, 1871 Frederiksberg, Denmark;* orcid.org/0000-0003-3486-271X

**Silas Anselm Rasmussen** − *Department of Biotechnology and Biomedicine, Technical University of Denmark, 2800 Kongens Lyngby, Denmark*

**Johan Ørskov Ipsen** − *Department of Plant and Environmental Sciences, Faculty of Science, University of Copenhagen, 1871 Frederiksberg, Denmark*

**Thomas Isbrandt** − *Department of Biotechnology and Biomedicine, Technical University of Denmark, 2800 Kongens Lyngby, Denmark;* orcid.org/0000-0003-3938-0816

**Thomas Ostenfeld Larsen** − *Department of Biotechnology and Biomedicine, Technical University of Denmark, 2800 Kongens Lyngby, Denmark;* orcid.org/0000-0002-3362-5707

Complete contact information is available at: https://pubs.acs.org/10.1021/acsomega.3c04299


### Author Contributions

P.K.B., N.T.J., T.O.L., and A.T.F. designed the research. S.A.R. and T.I. cultivated fungi and isolated fungal compounds. P.K.B., N.T.J., N.W.H., and J.Ø.I. did the research. T.O.L. and A.T.F. supervised the project. P.K.B. wrote the first draft of the manuscript with input from N.T.J., N.W.H., S.A.R., T.O.L., and A.T.F.

### Notes

The authors declare no competing financial interest.

## ■ ACKNOWLEDGMENTS

The authors acknowledge the financial support from The Danish Council for Independent Research, Technology, and Production Sciences (FTP) grant no. DFF-4184-00548 COMBAT, The Villum Foundation grant no. 35955, and the Carlsberg Foundation grant no. CF21-0389.

## ■ ABBREVIATIONS

ACMA, 9-amino-6-chloro-2-methoxyacridine; AlaM, alamethicin; CID, collision-induced dissociation; DLS, dynamic light scattering; DMSO, dimethyl sulfoxide; DPH, 1,6-diphenyl-1,3,5-hexatriene; ESI, electrospray ionization; IAA, indole-acetic acid; MEA, malt extract agar; PDA, potato dextrose agar; PM, plasma membrane; QTOF, quadrupole time-of-flight; RP-HPLC, reverse phase high-performance liquid chromatography; SLS, static light scattering; TMA-DPH, *N,N,N*-trimethyl-4-(6-phenyl-1,3,5-hexatrien-1-yl)phenylammonium; tPA II, trichorzin PA II; tPA VI, trichorzin PA VI; UHPLC−DAD−HRMS, ultrahigh-performance liquid chromatography−diode array detection−high-resolution mass spectrometry; YES, yeast extract with supplements

## ■ REFERENCES


(1) Savary, S.; Willocquet, L.; Pethybridge, S. J.; Esker, P.; McRoberts, N.; Nelson, A. The global burden of pathogens and pests on major food crops. *Nat. Ecol. Evol.* **2019**, *3* (3), 430−439.

(2) Secretariat I. P. P. C.. *Scientific Review of the Impact of Climate Change on Plant Pests − A Global Challenge to Prevent and Mitigate Plant Pest Risks in Agriculture, Forestry and Ecosystems*; FAO on behalf of the IPPC Secretariat, 2021.

(3) Weindling, R. *Trichoderma lignorum* as a parasite of other soil fungi. *Phytopathology* **1932**, *22* (10), 837−845.

(4) Harman, G. E.; Howell, C. R.; Viterbo, A.; Chet, I.; Lorito, M. Trichoderma species–opportunistic, avirulent plant symbionts. *Nat. Rev. Microbiol.* **2004**, *2* (1), 43−56.

(5) Nieto-Jacobo, M. F.; Steyaert, J. M.; Salazar-Badillo, F. B.; Nguyen, D. V.; Rostas, M.; Braithwaite, M.; De Souza, J. T.; Jimenez-Bremont, J. F.; Ohkura, M.; Stewart, A.; Mendoza-Mendoza, A. Environmental Growth Conditions of Trichoderma spp. Affects Indole Acetic Acid Derivatives, Volatile Organic Compounds, and Plant Growth Promotion. *Front. Plant Sci.* **2017**, *8*, No. 102.

(6) Sofo, A.; Scopa, A.; Manfra, M.; De Nisco, M.; Tenore, G.; Troisi, J.; Di Fiori, R.; Novellino, E. *Trichoderma harzianum* strain T-22 induces changes in phytohormone levels in cherry rootstocks (*Prunus cerasus* x *P. canescens*). *Plant Growth Regul.* **2011**, *65* (2), 421−425.

(7) Vinale, F.; Sivasithamparam, K.; Ghisalberti, E. L.; Marra, R.; Barbetti, M. J.; Li, H.; Woo, S. L.; Lorito, M. A novel role for Trichoderma secondary metabolites in the interactions with plants. *Physiol. Mol. Plant Pathol.* **2008**, *72* (1−3), 80−86.

(8) Stewart, A.; Hill, R. Applications of Trichoderma in Plant Growth Promotion. *Biotechnol. Biol. Trichoderma* **2014**, 415−428.

(9) Cafiso, D. S. Alamethicin - a Peptide Model for Voltage Gating and Protein Membrane Interactions. *Annu. Rev. Biophys. Biomol. Struct.* **1994**, *23*, 141−165.

(10) Vestergaard, M.; Christensen, M.; Hansen, S. K.; Gronvall, D.; Kjolbye, L. R.; Vosegaard, T.; Schiott, B. How a short pore forming peptide spans the lipid membrane. *Biointerphases* **2017**, *12* (2), No. 02d405.
(11) Abbasi, F.; Leitch, J. J.; Su, Z. F.; Szymanski, G.; Lipkowski, J. Direct visualization of alamethicin ion pores formed in a floating phospholipid membrane supported on a gold electrode surface. *Electrochim. Acta* **2018**, *267*, 195−205.
(12) Roversi, D.; Troiano, C.; Salnikov, E.; Giordano, L.; Riccitelli, F.; De Zotti, M.; Casciaro, B.; Loffredo, M. R.; Park, Y.; Formaggio, F.; et al. Effects of antimicrobial peptides on membrane dynamics: A comparison of fluorescence and NMR experiments. *Biophys. Chem.* **2023**, *300*, No. 107060.
(13) Kyle, K. E.; Puckett, S. P.; Caraballo-Rodriguez, A. M.; Rivera-Chávez, J.; Samples, R. M.; Earp, C. E.; Raja, H. A.; Pearce, C. J.; Ernst, M.; van der Hooft, J. J. J.; et al. *Trachymyrmex septentrionalis* ants promote fungus garden hygiene using Trichoderma-derived metabolite cues. *Proc. Natl. Acad. Sci. U. S. A.* **2023**, *120* (25), No. e2219373120.
(14) Marquette, A.; Bechinger, B. Biophysical Investigations Elucidating the Mechanisms of Action of Antimicrobial Peptides and Their Synergism. *Biomolecules* **2018**, *8* (2), No. 18.
(15) Kredics, L.; Szekeres, A.; Czifra, D.; Vagvolgyi, C.; Leitgeb, B. Recent Results in Alamethicin Research. *Chem. Biodiversity* **2013**, *10* (5), 744−771.
(16) Dotson, B. R.; Soltan, D.; Schmidt, J.; Areskoug, M.; Rabe, K.; Swart, C.; Widell, S.; Rasmusson, A. G. The antibiotic peptaibol alamethicin from Trichoderma permeabilises Arabidopsis root apical meristem and epidermis but is antagonised by cellulase-induced resistance to alamethicin. *BMC Plant Biol.* **2018**, *18*, No. 165.
(17) Lopez-Coria, M.; Hernandez-Mendoza, J. L.; Sanchez-Nieto, S. *Trichoderma asperellum* Induces Maize Seedling Growth by Activating the Plasma Membrane H+-ATPase. *Mol. Plant-Microbe Interact.* **2016**, *29* (10), 797−806.
(18) Lund, A.; Fuglsang, A. T. Purification of plant plasma membranes by two-phase partitioning and measurement of H+ pumping. *Methods Mol. Biol.* **2012**, *913*, 217−223.
(19) Bradford, M. M. A rapid and sensitive method for the quantitation of microgram quantities of protein utilizing the principle of protein-dye binding. *Anal. Biochem.* **1976**, *72*, 248−254.
(20) Kildgaard, S.; Mansson, M.; Dosen, I.; Klitgaard, A.; Frisvad, J. C.; Larsen, T. O.; Nielsen, K. F. Accurate Dereplication of Bioactive Secondary Metabolites from Marine-Derived Fungi by UHPLC-DAD-QTOFMS and a MS/HRMS Library. *Mar. Drugs* **2014**, *12* (6), 3681−3705.
(21) Baginski, E. S.; Foa, P. P.; Zak, B. Determination of Phosphate - Study of Labile Organic Phosphate Interference. *Clin. Chim. Acta* **1967**, *15* (1), 155−158.
(22) Wielandt, A. G.; Pedersen, J. T.; Falhof, J.; Kemmer, G. C.; Lund, A.; Ekberg, K.; Fuglsang, A. T.; Pomorski, T. G.; Buch-Pedersen, M. J.; Palmgren, M. Specific Activation of the Plant P-type Plasma Membrane $H^+$-ATPase by Lysophospholipids Depends on the Autoinhibitory N- and C-terminal Domains. *J. Biol. Chem.* **2015**, *290* (26), 16281−16291.
(23) Johansson, F.; Olbe, M.; Sommarin, M.; Larsson, C. Brij-58, a Polyoxyethylene Acyl Ether, Creates Membrane-Vesicles of Uniform Sidedness - a New Tool to Obtain inside-out (Cytoplasmic Side-out) Plasma-Membrane Vesicles. *Plant J.* **1995**, *7* (1), 165−173.
(24) Høiberg-Nielsen, R.; Fuglsang, C. C.; Arleth, L.; Westh, P. Interrelationships of glycosylation and aggregation kinetics for *Peniophora lycii* phytase. *Biochemistry* **2006**, *45* (15), 5057−5066.
(25) Duval, D.; Cosette, P.; Rebuffat, S.; Duclohier, H.; Bodo, B.; Molle, G. Alamethicin-like behaviour of new 18-residue peptaibols, trichorzins PA. Role of the C-terminal amino-alcohol in the ion channel forming activity. *Biochim Biophys Acta* **1998**, *1369* (2), 309−319.
(26) Alexandre, H.; Mathieu, B.; Charpentier, C. Alteration in membrane fluidity and lipid composition, and modulation of H +-ATPase activity in *Saccharomyces cerevisiae* caused by decanoic acid. *Microbiology* **1996**, *142*, 469−475.
(27) Grebowski, J.; Krokosz, A.; Puchala, M. Membrane fluidity and activity of membrane ATPases in human erythrocytes under the influence of polyhydroxylated fullerene. *Biochim. Biophys. Acta, Biomembr.* **2013**, *1828* (2), 241−248.
(28) Degenkolb, T.; Nielsen, K. F.; Dieckmann, R.; Branco-Rocha, F.; Chaverri, P.; Samuels, G. J.; Thrane, U.; von Dohren, H.; Vilcinskas, A.; Bruckner, H. Peptaibol, Secondary-Metabolite, and Hydrophobin Pattern of Commercial Biocontrol Agents Formulated with Species of the *Trichoderma harzianum* Complex. *Chem. Biodiversity* **2015**, *12* (4), 662−684.
(29) Contreras-Cornejo, H. A.; Macias-Rodriguez, L.; del-Val, E.; Larsen, J. Ecological functions of Trichoderma spp. and their secondary metabolites in the rhizosphere: interactions with plants. *FEMS Microbiol. Ecol.* **2016**, *92* (4), No. fiw036.
(30) Marik, T.; Tyagi, C.; Balazs, D.; Urban, P.; Szepesi, A.; Bakacsy, L.; Endre, G.; Rakk, D.; Szekeres, A.; Andersson, M. A.; et al. Structural Diversity and Bioactivities of Peptaibol Compounds From the Longibrachiatum Clade of the Filamentous Fungal Genus Trichoderma. *Front. Microbiol.* **2019**, *10*, No. 1434.
(31) Balázs, D.; Marik, T.; Szekeres, A.; Vagvolgyi, C.; Kredics, L.; Tyagi, C. Structure-activity correlations for peptaibols obtained from clade Longibrachiatum of Trichoderma: A combined experimental and computational approach. *Comput. Struct. Biotechnol. J.* **2023**, *21*, 1860−1873.
(32) Leitgeb, B.; Szekeres, A.; Manczinger, L.; Vagvolgyi, C.; Kredics, L. The history of alamethicin: A review of the most extensively studied peptaibol. *Chem. Biodiversity* **2007**, *4* (6), 1027−1051.
(33) Sansom, M. S. P. The Biophysics of Peptide Models of Ion Channels. *Prog. Biophys. Mol. Biol.* **1991**, *55* (3), 139−235.
(34) Benítez, T.; Rincón, A. M.; Limón, M. C.; Codon, A. C. Biocontrol mechanisms of Trichoderma strains. *Int. Microbiol.* **2004**, *7* (4), 249−260.
(35) Harman, G. E.; Howell, C. R.; Viterbo, A.; Chet, I.; Lorito, M. Trichoderma species - Opportunistic, avirulent plant symbionts. *Nat. Rev. Microbiol.* **2004**, *2* (1), 43−56.
(36) Pelagio-Flores, R.; Esparza-Reynoso, S.; Garnica-Vergara, A.; Lopez-Bucio, J.; Herrera-Estrella, A. Trichoderma-Induced Acidification Is an Early Trigger for Changes in Arabidopsis Root Growth and Determines Fungal Phytostimulation. *Front. Plant Sci.* **2017**, *8*, No. 822.
(37) Shi, W. L.; Chen, X. L.; Wang, L. X.; Gong, Z. T.; Li, S. Y.; Li, C. L.; Xie, B. B.; Zhang, W.; Shi, M.; Li, C. Y.; et al. Cellular and molecular insight into the inhibition of primary root growth of Arabidopsis induced by peptaibols, a class of linear peptide antibiotics mainly produced by Trichoderma spp. *J. Exp. Bot.* **2016**, *67* (8), 2191−2205.
(38) Aidemark, M.; Tjellstrom, H.; Sandelius, A. S.; Stalbrand, H.; Andreasson, E.; Rasmusson, A. G.; Widell, S. *Trichoderma viride* cellulase induces resistance to the antibiotic pore-forming peptide alamethicin associated with changes in the plasma membrane lipid composition of tobacco BY-2 cells. *BMC Plant Biol.* **2010**, *10*, No. 274.
(39) Bertelsen, K.; Vad, B.; Nielsen, E. H.; Hansen, S. K.; Skrydstrup, T.; Otzen, D. E.; Vosegaard, T.; Nielsen, N. C. Long-term-stable ether-lipid vs conventional ester-lipid bicelles in oriented solid-state NMR: altered structural information in studies of antimicrobial peptides. *J. Phys. Chem. B* **2011**, *115* (8), 1767−1774.
(40) Matic, S.; Geisler, D. A.; M?ller, I. M.; Widell, S.; Rasmusson, A. G. Alamethicin permeabilizes the plasma membrane and mitochondria but not the tonoplast in tobacco (*Nicotiana tabacum* L. cv Bright Yellow) suspension cells. *Biochem. J.* **2005**, *389*, 695−704.
(41) Dotson, B. R.; Soltan, D.; Schmidt, J.; Areskoug, M.; Rabe, K.; Swart, C.; Widell, S.; Rasmusson, A. G. The antibiotic peptaibol alamethicin from Trichoderma permeabilises Arabidopsis root apical meristem and epidermis but is antagonised by cellulase-induced resistance to alamethicin. *BMC Plant Biol.* **2018**, *18* (1), No. 165.


https://doi.org/10.1021/acsomega.3c04299
*ACS Omega* 2023, 8, 34928−34937

(42) Paweletz, L. C.; Holtbrügge, S. L.; Löb, M.; De Vecchis, D.; Schäfer, L. V.; Günther Pomorski, T.; Justesen, B. H. Anionic phospholipids stimulate the proton pumping activity of the plant plasma membrane P-type H+-ATPase *bioRxiv* 2023, DOI: 10.1101/2023.05.12.540525.
(43) Cazzola, R.; Della Porta, M.; Castiglioni, S.; Pinotti, L.; Maier, J. A. M.; Cestaro, B. Concentration-Dependent Effects of N-3 Long-Chain Fatty Acids on Na,K-ATPase Activity in Human Endothelial Cells. *Molecules* **2020**, *25* (1), No. 128.



https://doi.org/10.1021/acsomega.3c04299
*ACS Omega* 2023, 8, 34928−34937